ACS APPLIED MATERIALS & INTERFACES

Research Article

www.acsami.org

Assembly and Manipulation of Fe_3O_4/Coumarin Bifunctionalized Submicrometer Janus Particles

Yi-Cheng Chao, Wei-Hao Huang, Keng-Ming Cheng, and Changshu Kuo*

Department of Materials Science and Engineering, National Cheng Kung University, Tainan, 701-01, Taiwan

Supporting Information

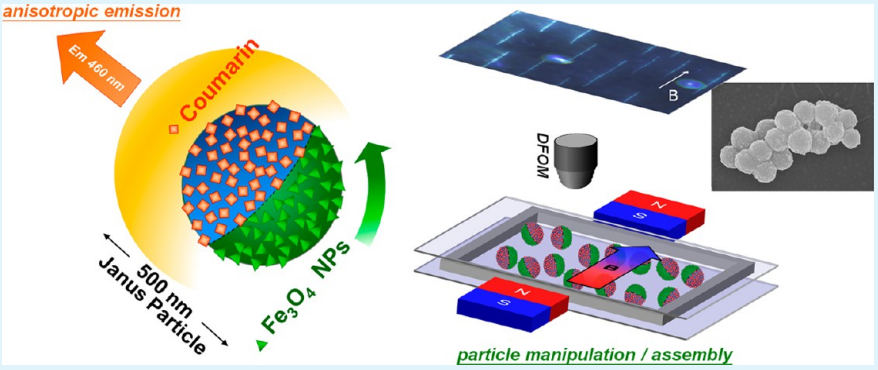

ABSTRACT: Magnetic and fluorescent bifunctionalized Janus particles were fabricated via sequential particle embedding and surface modifications. The two hemispherical surfaces of a 500 nm silica particle were separately functionalized with Fe_3O_4 nanoparticles and coumarin dye molecules. The Fe_3O_4 hemisphere exhibited magnetically driven particle orientation and alignment, whereas the coumarin hemisphere served as an anisotropic emission indicator. The photoluminescence of these orientated and solidified Janus particles revealed anisotropic emission contrast as high as 40% between the magnet-aspect and the dye-aspect excitations. The dynamic anisotropic emission of the bifunctionalized Janus suspension under magnetic manipulation also revealed a nonsynchronized bulk correlation time that was much slower than that of an individual 500 nm particle. Under a static magnetic field, the suspended Janus particles assembled into a grape-like bunch, with random particle orientation. Unlike their microscale counterparts, the submicrometer magnetic Janus particles were less sensitive to gravity and more vulnerable to particle−particle interactions.

KEYWORDS: *Janus particles, bifunctionalized, assembly, manipulation, magnetic, fluorescence, anisotropic, submicrometer particles*

INTRODUCTION

The assembly and manipulation of anisotropic micro- and nanomaterials have attracted increasing interest in recent years.[1,2] The anisotropicity of these materials results in unique building blocks with assembly behaviors that are unlike those of their isotropic or symmetric counterparts, whereas the multiple components simultaneously exhibit desired physical or chemical functionalities for other purposes. Among these candidates, the so-called Janus particle, a spherical object consisting of two distinct hemispheres, has attracted particular attention as a zero-dimensional anisotropic material.[3−5] Janus and Janus-like particles can be constructed using organic or inorganic materials, and their sizes range from several hundred micrometers down to a few nanometers in diameter. Other anisotropic materials that exhibit patchy,[6,7] triblock (ternary),[8,9] low-aspect-ratio (rods),[10] dumbbell,[11,12] and other specific shapes have also been synthesized and reported. Depending on the desired functionalities and morphologies, these asymmetric materials can be used in advanced applications, including assembled superstructures,[13,14] displays,[15] sensing devices,[16] imaging probes,[17] catalysis,[18] Pickering emulsions,[19] and suspension rheology.[20]

The assembly and manipulation of Janus particles involves intrinsic particle−particle interactions, as well as the external force applicable to an individual particle. The particle−particle interactions are usually determined by the functionality density and distribution, and the external force is typically proportional to the particle size (or mass). In most cases, larger particles are more sensitive to the gravity[10] caused by their own mass and may become relatively inert toward applied stimulation. Smaller particles, however, are more vulnerable to particle−particle interactions. With respect to external stimulation, Janus particles have been shown to respond to electric fields,[21,22] magnetic fields,[10,14,23,24] optomagnetic traps,[25] and self-propelling phenomena.[18,26]

Magnetically active Janus particles are an interesting subject that enable straightforward manipulation via switchable and

Received: January 2, 2014
Accepted: March 6, 2014
Published: March 6, 2014

   dx.doi.org/10.1021/am5000189 | ACS Appl. Mater. Interfaces 2014, 6, 4338−4345

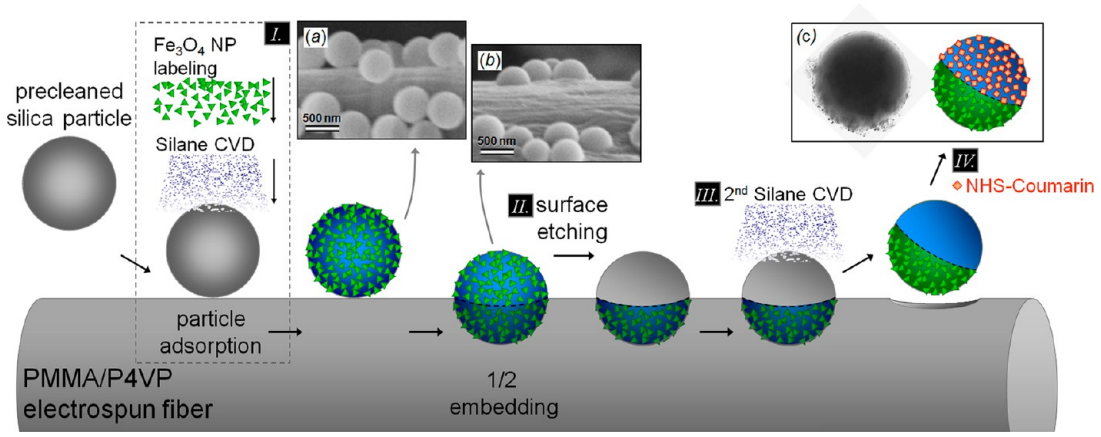

Figure 1. Fabrication method for Fe_3O_4/coumarin Janus particles. (a and b) SEM images of the silica particles on electrospun polymer fiber surfaces before and after embedding, respectively. (c) TEM image outlining the two hemispheres of a Janus particle.

adjustable regulation of both the direction and magnitude of the applied magnetic field. Magnetic hemispheres of Janus particles are usually introduced by the deposition of ferromagnetic coatings or by the selective attachment of magnetic nanoparticles. The core materials include polymers and ceramic colloids, and their diameters range from several micrometers to hundreds of micrometers.[8] The manipulation of these Janus microparticles is typically performed in a layer of a suspension, where the spatial confinement and particle diffusion are restricted in the vertical direction, i.e., the direction of gravity. The resulting particle assembly is moderately directed in the horizontal plane and forms assembled particle chains.

In this study, Janus particles cored with 500 nm silica were fabricated with two hemispheric surfaces individually functionalized with Fe_3O_4 nanoparticles and the fluorescent dye coumarin-466. These magnetic/coumarin Janus particles (MC-JPs) were further investigated on the basis of their anisotropic fluorescent emission as well as their magnetically driven particle orientation and alignment. The orientated and solidified MC-JP samples showed a high contrast in the anisotropic photoluminescence between the Fe_3O_4-aspect and the dye-aspect excitations. The MC-JP suspension was also sandwiched by two quartz slides using a 60 μm thick Surlyn sealing spacer. The spacer thickness was more than one hundred times larger than the MC-JP diameter to ensure particle assembly and alignment under the three-dimensional bulk environment. The manipulation of these submicrometer particles was monitored using dark-field optical microscopy (DFOM) in real time. Dynamic anisotropic photoluminescence revealed a relatively slow rotational correlation time from the nonsynchronized MC-JP rotation compared to that for an individual submicrometer particle. Under a static magnetic field (SMF), the MC-JPs in a suspension aligned as particle bunches parallel to the SMF direction. Real-time DFOM observations and other detailed analyses indicated that the magnetically driven assembly of submicrometer MC-JPs was vulnerable to particle Brownian motion and particle−particle interactions. The bunch morphologies and particle orientations were carefully examined using scanning electron microscopy (SEM), transmission electron microscopy (TEM), and scanning probe microscopy (SPM).

EXPERIMENTAL SECTION

Figure 1 illustrates the fabrication process of Fe_3O_4/coumarin bifunctionalized Janus particles, which is similar to the procedures described in a previous study.[8] In brief, the silica particles (500 ± 25 nm in diameter, Alfa Aesar) in an aqueous suspension were electrostatically attached to the surface of poly(methyl methacrylate)/poly(4-vinyl pyridine) (PMMA/P4VP) microfibers (average fiber diameter of 3 μm), which were fabricated via the electrospinning of PMMA and P4VP. The fiber scaffolds and attached silica particles were dried, and 3-aminopropyltrimethoxysilane was deposited by chemical vapor deposition (CVD) to generate the amino surface functionalities on the entire surface of the silica particles. Citrate-modified Fe_3O_4 nanoparticles (NPs),[8] which were also in an aqueous solution, were attached to the amino-enriched surfaces to complete the functionalization of the magnetic NPs (step I in Figure 1). For the following particle embedding process, the 50% submergence of Fe_3O_4-functionalized silica particles into the polymer fiber substrates was achieved using a 150 °C isothermal treatment for 4 h. This embedding temperature is higher than the 135 °C isothermal treatment used to stabilize the same 50% submerged silica particles with no surface modifications. The submerged Fe_3O_4-functionalized hemisphere was essentially protected, whereas the exposed top hemisphere was subject to remodification. The exposed Fe_3O_4 functionalities were etched with an aqueous NaOH solution (5 wt %) at room temperature, which removed the Fe_3O_4 NPs and amino-silanes from the exposed silica hemisphere. The PMMA/P4VP fiber scaffolds remained intact in this basic etching solution. The etching process was terminated by rinsing with deionized water several times until the pH of the washing solution became neutral. The same amino-silane CVD was subsequently performed a second time to generate fresh amino functionalities on the exposed silica hemispheres. These particles were then recovered by the dissolution of the polymer fiber scaffolds in an acetone/ethanol cosolvent (1:1 by volume), followed by centrifugal separation. Solvent washing and centrifugation were repeated four additional times to ensure complete removal of the excess Fe_3O_4 nanoparticles and polymer residues. Unlike the original white silica powder, the obtained sample was brown, presumably indicating the presence of Fe_3O_4 NPs.

The Janus particles with Fe_3O_4 and amino hemispheres were then reacted with NHS-functionalized coumarin-466 (*N*-succinimidyl ester coumarin-466; 7-(diethylamino)coumarin-3-carboxylic acid *N*-succinimidyl ester, from Sigma-Aldrich) in an acetonitrile solution at room temperature for 24 h. In a separated experiment, the successful coumarin grafting was monitored by the UV-vis spectra as a function of the reaction time between NHS-functionalized coumarin-466 and amino-Janus particles (see Supporting Information for details). Final purification via washing with acetonitrile solution and magnetically driven particle collection was performed. The unreacted dye molecules and silica particles containing no or low Fe_3O_4 NP loadings were separated. The purified Fe_3O_4/coumarin Janus particles were dried, weighed, and subsequently resuspended in an aqueous solution. This

dx.doi.org/10.1021/am5000189 | ACS Appl. Mater. Interfaces 2014, 6, 4338−4345

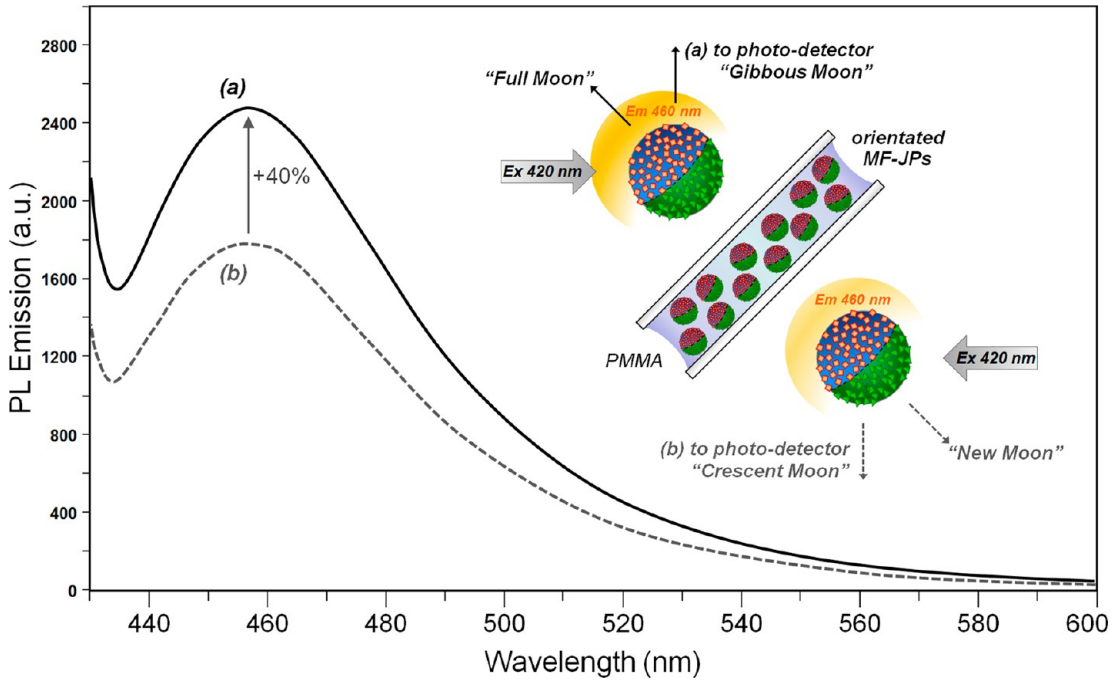

Figure 2. Anisotropic photoluminescence spectra of the solidified MC-JP/PMMA layer from (a) coumarin-aspect excitation (Full Moon) and (b) Fe_3O_4-aspect excitation (New Moon).

suspension was observed to be stable for several hours without precipitation.

RESULTS AND DISCUSSION

The successful fabrication of submicrometer Janus particles with desired bifunctionalities relies on uniform particle embedding during the isothermal treatment.[27] Therefore, the sequences of particle absorption and embedding on the polymer fiber surfaces were regularly monitored using SEM (see SEM images in Figure 1 and Supporting Information for sequential SEM images) to ensure a uniform degree of particle submerging after the isothermal treatment. Resulting functionality distribution on the Janus particle hemispheric surfaces had been determined to be more than 85% uniform in the prior work.[8] The magnetically driven particle collection during the final purification process excluded silica particles containing no or few attached Fe_3O_4 NPs. Upon UV irradiation, the effective coumarin grafting was also demonstrated by the intensive photoluminescence (PL) of the MC-JP suspension. Two distinct hemispheres of the final products were visually confirmed by TEM (see the inset TEM image in Figure 1), where the Fe_3O_4 nanoparticles outlined one hemispheric surface and the coumarin-functionalized hemisphere remained bald.

The anisotropic behavior of the MC-JPs was first demonstrated by their magnetically orientated encapsulation in a PMMA thin film. A methyl ethyl ketone (MEK) solution containing MC-JPs and PMMA was cast onto a quartz slide with a NdFeB magnet (approximately 120 mT at a close contact distance) positioned underneath it to facilitate the downward orientation of the Fe_3O_4 hemispheres. Before the solvent was completely evaporated, this sample was carefully sandwiched with another quartz slide (see the schematic sample assembly in the inset of Figure 2). MC-JP/PMMA solidification was ensured by storing this sandwiched sample and the underlying magnet in a vacuum chamber at room temperature for 12 h. This oriented MC-JP/PMMA thin layer appeared identical when observed from either side of the sandwiched quartz slides. However, the coumarin photoluminescence excited at 420 nm from two opposite aspects revealed a remarkable difference in the intensity of the 460 nm emission (see the two emission spectra in Figure 2). The coumarin-aspect excitation (nicknamed "Full Moon") resulted in an emission intensity 40% greater than that from the Fe_3O_4-aspect excitation (nicknamed "New Moon"). This anisotropic PL emission contrast was substantial compared to that observed in a prior investigation of bifunctionalized Janus particles constructed with Au NPs and Fe_3O_4 NPs on the two opposite hemispheres.[8] In that case, the transmittance UV-vis spectra of the similar encapsulated PMMA layer revealed Au NP surface plasmon resonance (SPR), with only a 6% anisotropic absorption contrast between both sides of the sandwiched sample. Notably, the anisotropic SPR absorption in the prior work occurred as incident light passed directly through the sample. However, the coumarin-aspect photoluminescence of the solidified MC-JP sample exhibited two anisotropic responses from both the irradiation absorption and the corresponding PL emission. The two anisotropic mechanisms subsequently established the greater optical contrast. Interestingly, the typical photoluminescence measurement was performed using excitation light with a 45° angle of incidence, and the emission was monitored by a photodetector also positioned at 45° with respect to the sample surface. From the vantage point of the photodetector, the "Full Moon" marked in Figure 2 was actually observed as a so-called "Gibbous Moon" and the "New Moon" was observed as a "Crescent Moon". Therefore, the intrinsic anisotropicity of the magnetically orientated MC-JP/PMMA thin layer was believed to be greater than the 40% emission contrast, as observed in the PL measurements.

The magnetically induced MC-JP orientation and the anisotropic PL emission were also investigated as functions of

dx.doi.org/10.1021/am5000189 | ACS Appl. Mater. Interfaces 2014, 6, 4338−4345

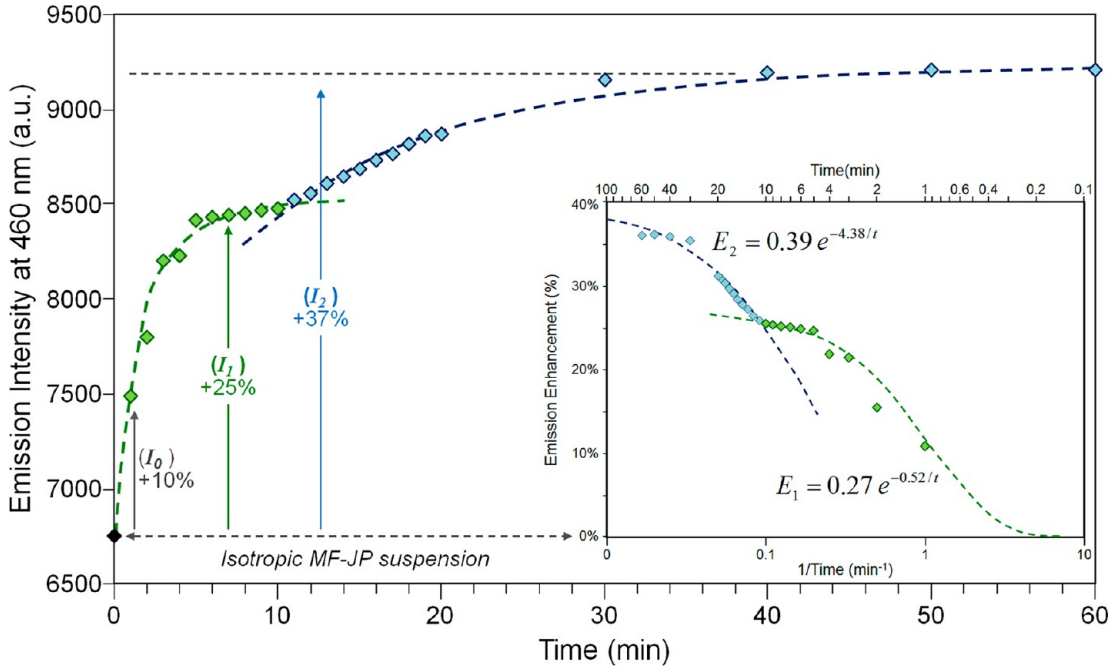

Figure 3. Dynamic anisotropic photoluminescence of a MC-JP suspension under magnetic induction. In the inset, the emission intensity versus the reciprocal of time is plotted together with two exponential curve fittings.

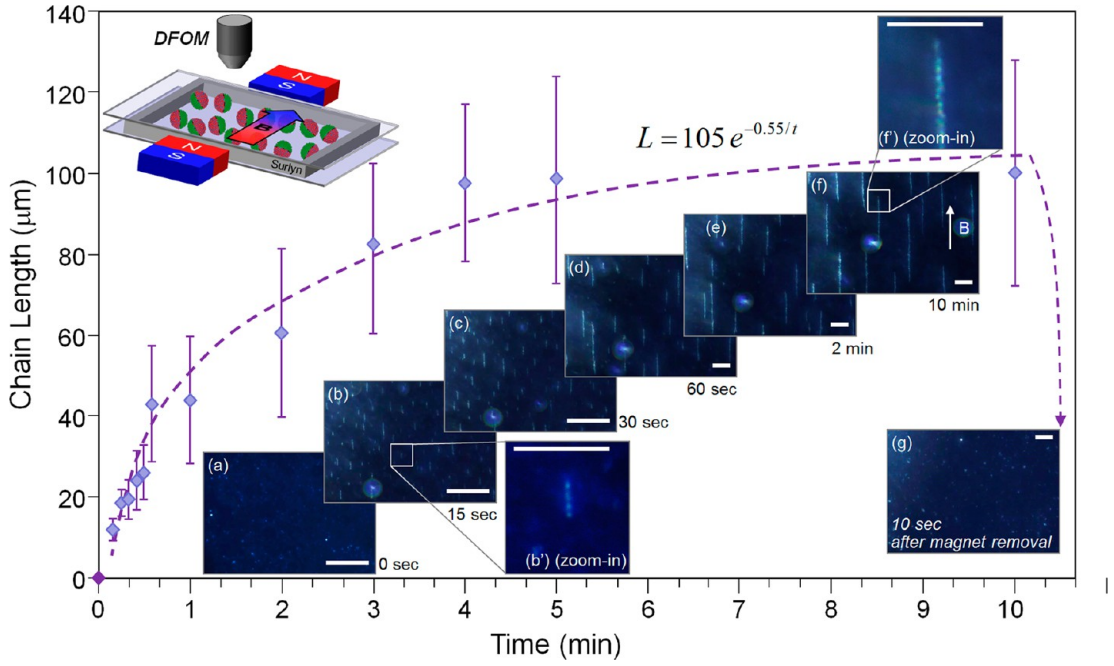

Figure 4. Dynamic MC-JP alignment and the consequent chain length growth under a static magnetic field.

time. A MC-JP aqueous suspension with an approximate concentration of 1×10^{-3} (by weight) was sealed between one wafer and one quartz slide using a Surlyn sealing spacer (60 μm in thickness). In this dilute suspension concentration, the average particle−particle distance was estimated to be approximately 7 μm, which is approximately 14 times larger than the 500 nm particle diameter. This particle−particle distance also supported approximately nine particles on average in the vertical distribution of the 60 μm spacing. The sealed sample was mounted in the photoluminescence spectrometer with the quartz slide at a 45° angle facing the excitation source.

The emission spectrum of the as-sealed MC-JP suspension under 420 nm excitation was first recorded as the isotropic emission baseline. When the NdFeB magnet was positioned near the sample (behind the wafer), it instantly stimulated the 460 nm emission with an intensity increase of more than 10% within 1 min (marked as I_0 in Figure 3), followed by the first saturation in 5 min at an emission elevation of approximately 25% (marked as phase I_1). Subsequently, the emission intensity increased again at 10 min after the magnet was positioned (marked as phase I_2) and reached a final maximum 37% greater than the initial emission intensity of the as-sealed isotropic

dx.doi.org/10.1021/am5000189 | ACS Appl. Mater. Interfaces 2014, 6, 4338−4345

sample. In the inset of Figure 3, the emission intensity under magnetic induction is plotted versus the reciprocal of the time. Here, the phase I_1 emission increase as a function of time was fitted with the exponential curve $E_1 = 0.27^{e-0.52/t}$, and the phase I_2 emission profile was fitted with the exponential relationship $E_2 = 0.39e^{-4038/t}$. Equation E_1, with the shorter correlation time (τ_1) of 0.52 min (or 31 s), indicated that phase I_1 underwent a faster response than did phase I_2, where equation E_2 had a correlation time (τ_2) of 4.38 min. The rotational correlation time of a 500 nm particle in an aqueous medium has been theoretically estimated to be 0.05 s.[28] Direct optical observation of a 2 μm magnetic Janus particle has also been used to determine that the particle rotational correlation time is as fast as 2.26 s.[29] Accordingly, the rotation of a single MC-JP in an aqueous suspension was expected to have a correlation time that matched phase I_0 instead of phase I_1 (31 s) or phase I_2 (4.38 min). Because particle−particle interactions in the dilute MC-JP suspension had been eliminated, the independent particle motion under the applied magnetic field did not support the synchronization of particle rotation. Whereas the directional magnetic force encountered random particle Brownian motion, the phase oscillation from individual MC-JP rotation prolonged the saturation of the anisotropic PL emission dramatically, as indicated by correlation time τ_1. The 31 s rotation correlation time for the bulk MC-JP suspension was observed to be much slower than that for an individual 500 nm particle.

In contrast, the phase I_2 emission growth was assigned to the migration of the suspended particle toward the magnet. The drifting and precipitation of the MC-JP toward the substrate surface completely eliminated the particle Brownian motion and gradually secured the anisotropic emission. During this stage, the particle−particle distance was shortened. Therefore, an interaction between two magnetic Janus particles was highly likely. Within approximately 30 min, the saturation of the emission intensity at a level as much as 37% greater than the emission intensity of the isotropic sample indicated that most of the MC-JPs had drifted across the 60 μm gap within the sandwiched sample. Notably, it was observed that mild sonication caused the resuspension of most of the precipitated MC-JPs. Under the same magnetic manipulation, the anisotropic PL emission profile shown in Figure 3 was repeatable, with a minor decrease in PL intensity.

The magnetically driven migration of the suspended MC-JP can be constrained using a static magnetic field (SMF), i.e., a negligible gradient in the magnetic flux density. Under SMF induction, the magnetic Janus materials underwent particle assembly and alignment.[30,31] As illustrated in Figure 4, two NdFeB magnets were placed laterally on opposite sides of the MC-JP suspension, sandwiched by two quartz slides. The uniform SMF of approximately 38 mT was changed through adjustment of the distance between the two magnets. Dark-field optical microscopy (DFOM) was to monitor the submicrometer MC-JPs in real time. The DFOM images of the as-sealed suspension showed randomly distributed spots that indicated the population of MC-JPs under Brownian motion (see inset image a in Figure 4). The approach of two lateral magnets immediately induced particle alignment as chained spots. The 15 s DFOM image (inset b in Figure 4) revealed that the MC-JP alignment increased the chain length by an average of approximately 12 μm. At this moment, these growing chains were still surrounded by numerous individual particles (the isolated spots in the image). The individual particles, along with other short particle chains, progressively drifted and joined the longer particle parades, as observed in the sequential DFOM images (insets a to f in Figure 4). All the MC-JP chains were aligned parallel to each other in the direction of the SMF. No other aggregation forms or particle alignment directions were observed. Two magnified DFOM images (b′ and f′ in Figure 4) show the particle alignments after 15 s and 10 min of SMF induction, respectively, where the connected MC-JPs in the alignment were individually identified as chained spots. The MC-JP alignments in the DFOM images were recorded as a function of time, and they reached the saturated chain length of approximately 100 μm in 4 min. The absence of individual spots in DFOM image f in Figure 4 also indicates the consumption of isolated MC-JPs.

Because the MC-JPs were functionalized with paramagnetic nanoscale Fe_3O_4 particles, both magnetization and demagnetization were nearly instantaneous (magnetization curves available in the Supporting Information). The removal of the two parallel magnets led to the immediate collapse of the particle alignment (see inset image g in Figure 4). This result suggested that the SMF induction of each MC-JP occurred instantly and that the formation of the particle alignment was slowed by the diffusion of individual particles and short particle chains. In addition, the maximum length of the particle alignments was determined by the particle concentrations in the suspension. The chain length profile as a function of time (the purple curve in Figure 4) was fitted with an exponential curve $L = 105e^{-0.55/t}$, where the assembly correlation time (τ_L) of 0.55 min (or 33 s) reflected MC-JP diffusion and alignment under SMF induction. The ratio between the average particle−particle distance (7 μm) in this particular suspension concentration and the assembly correlation time (τ_L = 0.55 min) determined from Figure 4 was calculated to be 12.7 μm/min (7 μm/0.55 min), which corresponds to the average MC-JP diffusion rate. In contrast to the phase I_2 correlation time corresponding to a MC-JP drifting to one magnet (Figure 3), that of particle migration through the 60 μm Surlyn was τ_2 = 4.38 min, whereas the magnitude of the corresponding diffusion rate of 13.6 μm/min (60 μm/4.38 min) was similar. These results suggest that the diffusion rates of the MC-JP suspension remained approximately the same for both the lengthy migration toward one magnet and the short distance diffusion in the SMD-induced particle alignment.

The SMF-induced particle alignment was further analyzed on the basis of the solidification of these particle parades. The sandwiched suspension was replaced with the MC-JP solution cast directly onto a wafer substrate precoated with a thin PMMA layer (approximately 200 nm in thickness). Similar to the previously discussed case of the encapsulated sample, sample solidification was accompanied by the presence of the two laterally opposite magnets. The concentration of the aqueous MC-JP suspension was maintained at approximately 1 $\times 10^{-3}$ wt %, which was the same as the concentration of the sandwiched sample. In addition, the magnet fields were adjusted to approximately 10, 15, and 38 mT by varying the distances between the two magnets. After the water was evaporated, the magnets were removed, and the sample was isothermally treated at 100 °C for 10 min. The moderate softening of the PMMA thin underlayer at this temperature slightly embedded the 500 nm silica particles, which prevented possible particle relocation during the morphology measurement, especially during scanning probe microscopy (SPM). The immobilized particle alignments were first examined using

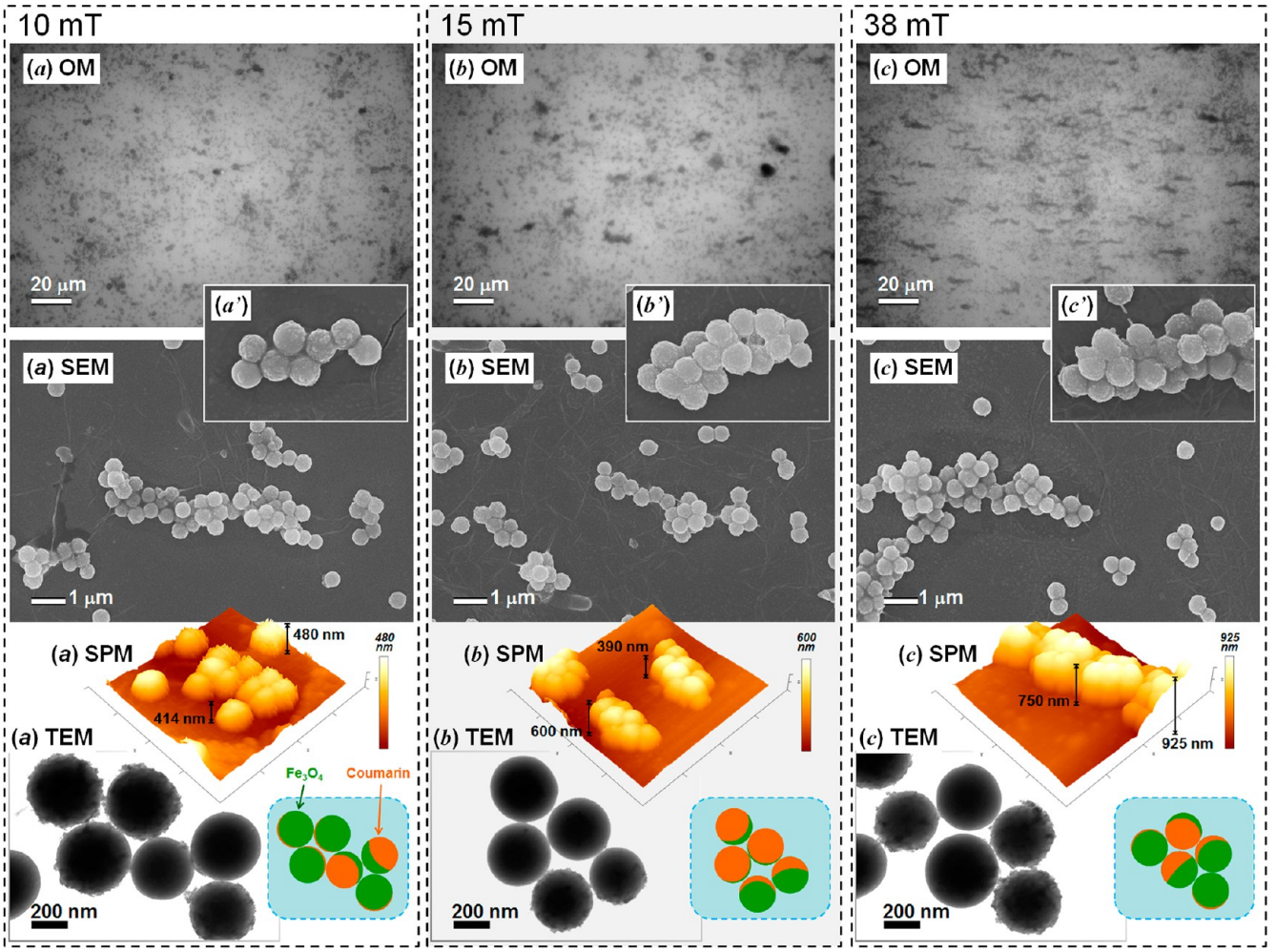

Figure 5. The morphologies of the MC-JP alignments under (a) 10, (b), 15, and (c) 38 mT SMFs were analyzed using OM, SEM, SPM, and TEM.

an optical microscope (OM) under ambient light. Under the same 38 mT SMF induction, the chain lengths of the solidified MC-JP (Figure 5c) barely reached 30 μm, which is much shorter than the 100 μm particle assembly in the suspension sample shown in Figure 4. In addition, a considerable number of smaller clusters surround the short particle chains in both the OM and SEM images (Figure 5c′). It was believed that the solution condensation and the water surface tension during the drying process interrupted the particle parades,[31] which resulted in the shortening of the alignment and chain breaking. Nevertheless, these solidified samples permitted detailed observations of the submicrometer Janus particles, including the assembly morphology and the particle orientation.

Under SMF-induction, the MC-JP alignments were observed to be different from the staggered or zigzag particle assemblies observed in the micrometer-scale magnetic Janus particles (diameters between 10 and 100 μm).[30,31] Herein, the submicrometer MC-JP sample contained grape-like particle bunches, as shown in the SEM images (Figure 5). Although a few zigzag-arranged MC-JPs were also isolated in the 10 mT SMF sample (see magnified SEM image, Figure 5a′), most of the MC-JP alignments were identified as grape-like bunches with three or more particles in their cross-section (Figure 5b′,c′). These SEM images also indicated that a stronger SMF encouraged the formation of thicker particle bunches. The three-dimensional morphologies of these particle bunches were sketched by the SPM measurements. Under 10, 15, and 38 mT SMF inductions, the heights of the partially embedded particles were measured to be between 390 and 925 nm (see the SPM mappings in Figure 5). With respect to the 200 nm thickness of the PMMA underlayer, the SPM topographies indicated that the particle bunches were constructed by one to three 500 nm MC-JPs in a bunch cross-section, in agreement with the SEM two-dimensional observations.

The orientations of individual MC-JPs in the assembled bunch were examined by TEM measurements. The MC-JP suspension solutions were carefully deposited on TEM sample grids in the presence of two laterally opposite magnets, similar to the sample preparation procedure described previously. A small amount of poly(ethylene glycol) (PEG) was added to the MC-JP aqueous suspension to secure the particle alignment during and after the water evaporation process. Because of the considerable thickness of the silica particle bunches, the TEM images in Figure 5 only show selected zigzag-arranged particle assemblies under three SMF magnitudes. The colored sphere sketches to the right of these TEM images represent the Fe_3O_4 and coumarin hemispheres in green and orange, respectively. Herein, the Fe_3O_4 hemispheres of MC-JP were observed to be randomly oriented, without a specific orientation preference, unlike the alignment of the micrometer-scale Janus particles with the unique inward orientation of the magnetic hemispheres.[10,30,31]

dx.doi.org/10.1021/am5000189 | ACS Appl. Mater. Interfaces 2014, 6, 4338−4345

For the assembly of micrometer-scale Janus particles, the gravity effect is an inevitable issue. The stability of a dimer or a larger cluster of particles may require a specific arrangement of the magnetic hemispheres; otherwise, the gravity force can easily overwhelm the relatively weak particle−particle interactions. Additional assembly controls have been frequently achieved through certain spatial confinement to the Janus particle suspension, particularly in the gravity direction. With less dimensional freedom, the specific hemisphere arrangement encourages the formation of staggered or zigzag particle assemblies. In the case of the submicrometer MC-JPs, however, the gravity effect was substantially downgraded due to the reduction in the particle diameter and mass. The particle−particle paramagnetic interactions easily dominated the assembly mechanism, without the need for a specific magnetic hemisphere arrangement. The resulting particle alignment exhibited random particle orientation and bunch morphology.

CONCLUSION

Submicrometer-scale silica particles were successfully bifunctionalized with two hemispheres of magnetic Fe_3O_4 nanoparticles and fluorescent coumarin molecules. These unique bifunctionalized Janus particles simultaneously exhibited magnetically induced orientation and anisotropic fluorescent emission. The magnetically manipulated Janus particles were monitored and analyzed on the basis of the anisotropic emission intensity. Time-dependent emission measurements suggested that the magnetically induced rotation of the suspended MC-JPs was slowed by the original Brownian particle motion and by the lack of a particle synchronization mechanism. SMF-induced particle alignment for the submicrometer-scale magnetic Janus particles resulted in a grape-like particle bunch, with no orientation preference for the magnetic hemispheres. The submicrometer magnetic Janus particles were also demonstrated to be less sensitive to the gravity effect and more vulnerable to desirable particle−particle interactions.

ASSOCIATED CONTENT

Supporting Information

NHS-functionalized coumarin-466 grafting reaction on the amino Janus particles, SEM images for the fabrication sequences, the magnetization curves, and the TEM and SPM images with high resolution. This material is available free of charge via the Internet at http://pubs.acs.org.

AUTHOR INFORMATION

Corresponding Author

*E-mail: changshu@mail.ncku.edu.tw.

Notes

The authors declare no competing financial interest.

ACKNOWLEDGMENTS

The authors are grateful for the financial support received from the National Science Council (NSC 101-2221-E-006-133 and NSC 102-2221-E-006-074). Prof. Ingann Chen at National Cheng Kung University is also acknowledged for assistance with the magnetic field measurements and for helpful discussions.

REFERENCES

(1) Murphy, C. J.; Sau, T. K.; Gole, A. M.; Orendorff, C. J.; Gao, J.; Gou, L.; Hunyadi, S. E.; Li, T. Anisotropic Metal Nanoparticles: Synthesis, Assembly, and Optical Applications. *J. Phys. Chem. B* **2005**, *109*, 13857−13870.

(2) Yoshida, M.; Lahann, J. Smart Nanomaterials. *ACS Nano* **2008**, *2*, 1101−1107.

(3) Lattuada, M.; Hatton, T. A. Synthesis, Properties and Applications of Janus Nanoparticles. *Nano Today* **2011**, *6*, 286−308.

(4) Kaewsaneha, C.; Tangboriboonrat, P.; Polpanich, D.; Eissa, M.; Elaissari, A. Janus Colloidal Particles: Preparation, Properties, and Biomedical Applications. *ACS Appl. Mater. Interfaces* **2013**, *5*, 1857−1869.

(5) Kaewsaneha, C.; Tangboriboonrat, P.; Polpanich, D.; Eissa, M.; Elaissari, A. Preparation of Janus Colloidal Particles via Pickering Emulsion: An Overview. *Colloids Surf., A* **2013**, *439*, 35−42.

(6) McConnell, M. D.; Kraeutler, M. J.; Yang, S.; Composto, R. J. Patchy and Multiregion Janus Particles with Tunable Optical Properties. *Nano Lett.* **2010**, *10*, 603−609.

(7) Pawar, A. B.; Kretzschmar, I. Fabrication, Assembly, and Application of Patchy Particles. *Macromol. Rapid Commun.* **2010**, *31*, 150−168.

(8) Lin, C.-C.; Liao, C.-W.; Chao, Y.-C.; Kuo, C. Fabrication and Characterization of Asymmetric Janus and Ternary Particles. *ACS Appl. Mater. Interfaces* **2010**, *2*, 3185−3191.

(9) Chen, Q.; Bae, S. C.; Granick, S. Directed Self-Assembly of a Colloidal Kagome Lattice. *Nature* **2011**, *469*, 381−384.

(10) Yan, J.; Chaudhary, K.; Bae, S. C.; Lewis, J. A.; Granick, S. Colloidal Ribbons and Rings from Janus Magnetic Rods. *Nat. Commun.* **2013**, *4*, 1516.

(11) Pradhan, S.; Ghosh, D.; Chen, S. Janus Nanostructures Based on Au-TiO_2 Heterodimers and Their Photocatalytic Activity in the Oxidation of Methanol. *ACS Appl. Mater. Interfaces* **2009**, *1*, 2060−2065.

(12) Elsukova, A.; Li, Z.-A.; Moeller, C.; Spasova, M.; Acet, M.; Farle, M.; Kawasaki, M.; Ercius, P.; Duden, T. Structure, Morphology, and Aging of Ag-Fe Dumbbell Nanoparticles. *Phys. Status Solidi A* **2011**, *208*, 2437−2442.

(13) Jiang, S.; Chen, Q.; Tripathy, M.; Luijten, E.; Schweizer, K. S.; Granick, S. Janus Particle Synthesis and Assembly. *Adv. Mater.* **2010**, *22*, 1060−1071.

(14) Yan, J.; Bloom, M.; Bae, S. C.; Luijten, E.; Granick, S. Linking Synchronization to Self-Assembly Using Magnetic Janus Colloids. *Nature* **2012**, *491*, 578−581.

(15) Yin, S.-N.; Wang, C.-F.; Yu, Z.-Y.; Wang, J.; Liu, S.-S.; Chen, S. Versatile Bifunctional Magnetic-Fluorescent Responsive Janus Supraballs Towards the Flexible Bead Display. *Adv. Mater.* **2011**, *23*, 2915−2919.

(16) Lee, J.; Kim, J. Multiphasic Sensory Alginate Particle Having Polydiacetylene Liposome for Selective and More Sensitive Multitargeting Detection. *Chem. Mater.* **2012**, *24*, 2817−2822.

(17) Sotiriou, G. A.; Hirt, A. M.; Lozach, P.-Y.; Teleki, A.; Krumeich, F.; Pratsinis, S. E. Hybrid, Silica-Coated, Janus-Like Plasmonic-magnetic Nanoparticles. *Chem. Mater.* **2011**, *23*, 1985−1992.

(18) Baraban, L.; Makarov, D.; Streubel, R.; Monch, I.; Grimm, D.; Sanchez, S.; Schmidt, O. G. Catalytic Janus Motors on Microfluidic Chip: Deterministic Motion for Targeted Cargo Delivery. *ACS Nano* **2012**, *6*, 3383−3389.

(19) Fan, H.; Resasco, D. E.; Striolo, A. Amphiphilic Silica Nanoparticles at the Decane-Water Interface: Insights from Atomistic Simulations. *Langmuir* **2011**, *27*, 5264−5274.

(20) Park, B. J.; Lee, D. Equilibrium Orientation of Nonspherical Janus Particles at Fluid-Fluid Interfaces. *ACS Nano* **2012**, *6*, 782−790.

(21) Gangwal, S.; Cayre, O. J.; Velev, O. D. Dielectrophoretic Assembly of Metallodielectric Janus Particles in AC Electric Fields. *Langmuir* **2008**, *24*, 13312−13320.

(22) Zhang, L.; Zhu, Y. Directed Assembly of Janus Particles under High Frequency AC-Electric Fields: Effects of Medium Conductivity and Colloidal Surface Chemistry. *Langmuir* **2012**, *28*, 13201−13207.

(23) Dyab, A. K. F.; Ozmen, M.; Ersoz, M.; Paunov, V. N. Fabrication of Novel Anisotropic Magnetic Microparticles. *J. Mater. Chem.* **2009**, *19*, 3475−3481.

(24) Smoukov, S. K.; Gangwal, S.; Marquez, M.; Velev, O. D. Reconfigurable Responsive Structures Assembled from Magnetic Janus Particles. *Soft Matter* **2009**, *5*, 1285−1292.
(25) Erb, R. M.; Jenness, N. J.; Clark, R. L.; Yellen, B. B. Towards Holonomic Control of Janus Particles in Optomagnetic Traps. *Adv. Mater.* **2009**, *21*, 4825−4829.
(26) Wu, Y.; Wu, Z.; Lin, X.; He, Q.; Li, J. Autonomous Movement of Controllable Assembled Janus Capsule Motors. *ACS Nano* **2012**, *6*, 10910−10916.
(27) Ho, C.-C.; Chen, W.-S.; Shie, T.-Y.; Lin, J.-N.; Kuo, C. Novel Fabrication of Janus Particles from the Surfaces of Electrospun Polymer Fibers. *Langmuir* **2008**, *24*, 5663−5666.
(28) Behrend, C. J.; Anker, J. N.; McNaughton, B. H.; Brasuel, M.; Philbert, M. A.; Kopelman, R. Metal-Capped Brownian and Magnetically Modulated Optical Nanoprobes (MOONs): Micromechanics in Chemical and Biological Microenvironments. *J. Phys. Chem. B* **2004**, *108*, 10408−10414.
(29) McNaughton, B. H.; Kinnunen, P.; Shlomi, M.; Cionca, C.; Pei, S.-N.; Clarke, R.; Argyrakis, P.; Kopelman, R. Experimental System for One-Dimensional Rotational Brownian Motion. *J. Phys. Chem. B* **2011**, *115*, 5212−5218.
(30) Yuet, K. P.; Hwang, D. K.; Haghgooie, R.; Doyle, P. S. Multifunctional Superparamagnetic Janus Particles. *Langmuir* **2009**, *26*, 4281−4287.
(31) Ren, B.; Ruditskiy, A.; Song, J. H.; Kretzschmar, I. Assembly Behavior of Iron Oxide-Capped Janus Particles in a Magnetic Field. *Langmuir* **2012**, *28*, 1149−1156.